Study of fault zone damage and healing in the 2019 Ridgecrest aftershock sequence

John E. Vidale (PI), Wei Wang (co-PI)

Department of Earth Sciences, University of Southern California

Reference: SCEC #20111

Abstract

Tectonic faults, as zones of weakness, are central to plate tectonics. By velocity weakening and strain localization, faults generate earthquakes from plate motions. One outstanding question is just how faults weaken as they break, and then restrengthen afterwards. Faults may heal through a variety of deformation processes; closure of cracks by indentation, sealing of cracks by chemical processes, or redistribution of fluids, for example. The 2019 M7.1 Ridgecrest earthquake and its M6.4 foreshock occurred near the town of Ridgecrest on July 5 and were the first such strong events in southern California for 20 years. Numerous individual stations and fault crossing arrays were recorded as a community resource, providing unprecedented measurements in the ensuing weeks. We examined the repeating earthquakes [*Trugman et al.*, 2020] to identify the changes in seismic wave speed. We use the travel time difference of P and S waves using the repeating events to measure the velocity changes of the fault zone and wallrock. Our results resolve the NW-ES-oriented main fault below the linear array B3 has a width of 1.2 km, and a second, perpendicular fault is not as clear but has the width about 0.8 km. We only detect a subtle healing process only within the fault zone, i.e. less than 1% shear-wave velocity increased during the less than one-month period of the array working. This study provides knowledge of the fault zone structure and the earthquake cycle for the 2019 M7.1 Ridgecrest earthquake.

Intellectual Merit

The performed results measure the fault zone healing process of the faults for the M7.1 Ridgecrest mainshock and the M6.5 foreshock. Also, the results reveal the fault widths for the main fault and a perpendicular one. The stronger healing processing for S wave in the fault zone rather than for P wave or in the wallrock indicates fluids may be involved in the healing process.

Broader Impacts

This research provides important constraints on fault zone structure. The nonlinear behavior of the material within the fault zone is key to understand the earthquake cycling and nucleation. The differences in healing process for P and S wave may indicate the influence of the fluid in fault weakening and the earthquake cycling. These discoveries are important to the rock mechanics and laboratory experiments.

Preliminary Results

The repeating earthquakes are events occurring almost at the same place but at different time. The same occurrence location assures they have almost the same raypath, making them an effective tool to detect the changes of the media along the raypath. The dense aftershock sequence of M7.1 Ridgecrest earthquake has been interrogated by new detection and relocation methods, providing a catalog of many thousands of precisely located aftershocks to probe the

fault and surrounding crust, with thousands of repeating events identified [*Trugman et al.*, 2020]. After M7.1 Ridgecrest earthquake, teams from the University of Utah, UC Riverside, the USGS, and others deployed numerous seismometers, many in cross-fault linear arrays (see Figure 1).

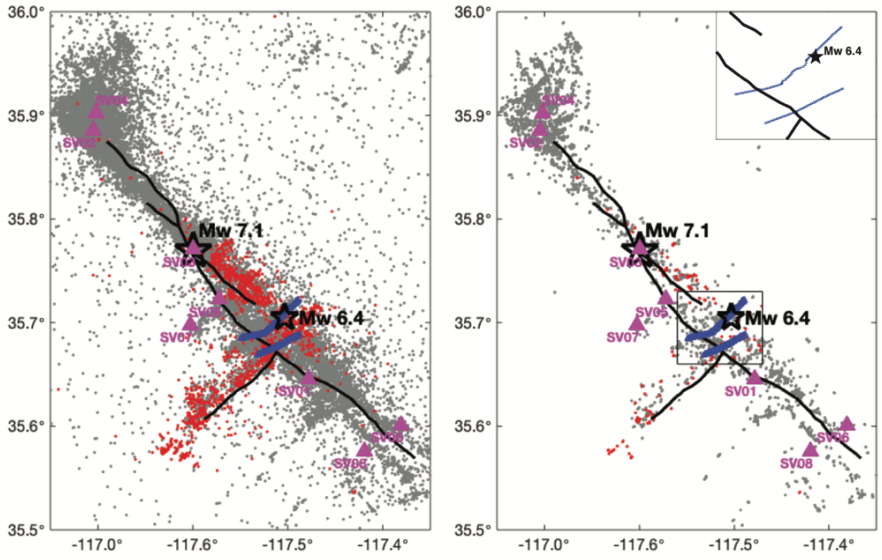

Figure 1. (Left) Map of the 2019 Ridgecrest earthquakes (foreshock and mainshock), aftershocks (to 2019/08/28), near-fault stations (magenta) and two of the nodal arrays (blue). The red dots mark the aftershocks of the M6.4 foreshock before the M7.1 mainshock. The grey dots are the locations of the aftershocks for the M7.1 mainshock. The fault plane is derived from InSAR [*Xu et al.*, 2020]. (Right) Map with the repeating earthquake locations [*Trugman et al.*, 2020].

Linear Array Analysis

In this study, we examined the velocity changes based on those two seismic arrays using repeating event clusters, aimed to seek velocity healing within the fault zone (FZ). To resolve the FZ healing process, we choose the clusters containing more than 4 events with magnitude larger than 1 and the time span longer than 15 days. The waveform similarity of the repeating clusters is sensitive to the relative locations between events. We only use the clusters with relative location differences smaller than 100 meters. Furthermore, the cross-correlation (CC) coefficients are required to be larger than 0.9 for P-wave, S-wave and whole seismograms of the repeating event pairs to assure the similarity of the repeating event clusters. The P and S wave arrival times are predicted using PSIRpicker [*Li and Peng*, 2016].

The stations located across FZs would best image the velocity change within FZ. Our best repeater multiplets indicate the linear array B3 was deployed across two faults, as identified below by zones of healing. The NW-ES-oriented main fault has a width of 1.2 km, and the second, perpendicular fault is not as clear but has the width about 0.8 km. These results are consistent with results from a teleseismic P wave study [see *Qiu et al.*, 2020]. Since the dense arrays were only working for less than one month and started one week after the M7.1 mainshock, the healing process is faint (< 1%), and likely represented only a fraction of the healing across the entire earthquake cycle. The fault zone shows stronger healing than wall rocks and S waves stronger healing than P waves, which may indicate fluid fills the opened cracks [*Schaff and Beroza*, 2004].

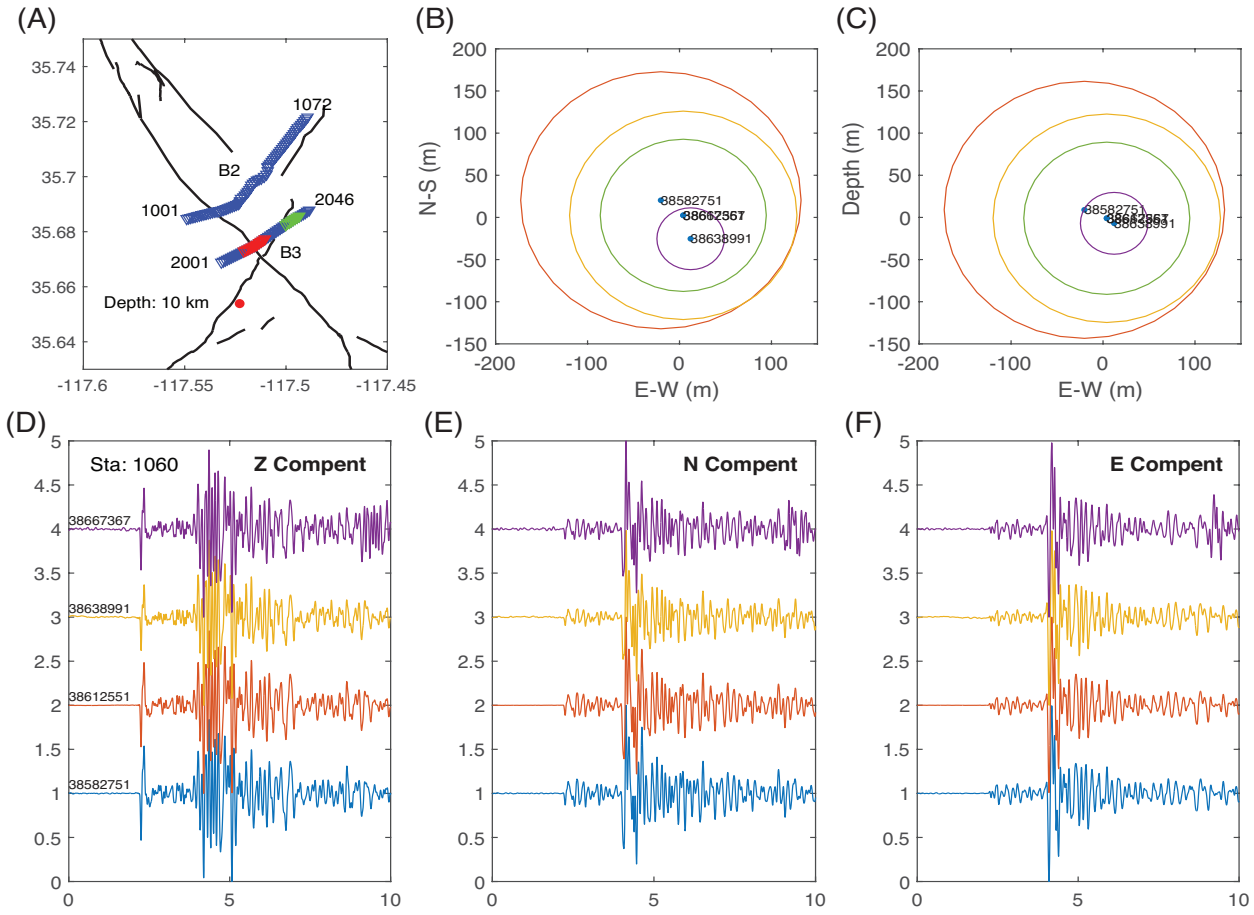

Figure 2. (A) Location of the repeaters (red dot) and two dense arrays. The triangles mark the individual stations of the two dense arrays. The red and green sections highlight the detected fault zones. (B) and (C) show the relative locations of the four repeating events with their rupture areas assuming the Brune-type rupture model with stress drop 3 MPa. (D)-(F) shows the seismograms of different components aligning at the occurrence time for the four repeating events.

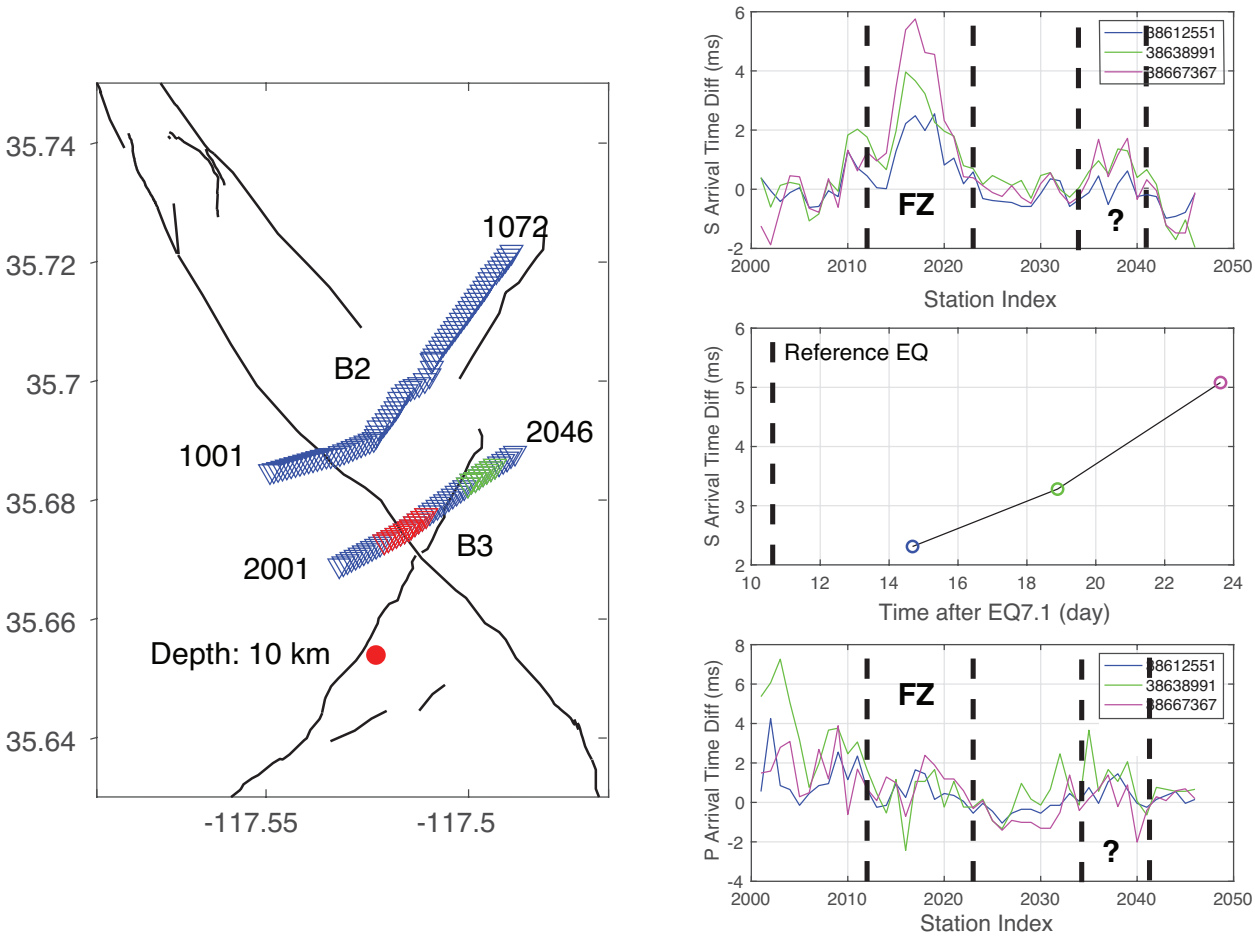

Figure 3. (A) Location of the repeaters (red dot) and two dense arrays. The triangles mark the individual stations of the two dense arrays. The red and green sections highlight the detected fault zones. (B) P wave arrival time delays relative to the earliest event (38582751) along the southern dense array (B3 in A). (C) S wave arrival time delays relative to the earliest event along the southern dense array in Figure 2A. The inferred fault zones are delimited by black dashed lines. (D) illustrates the average S arrival time delay within the fault zone marked in (B) and (C) versus to the occurrence time relative to the M7.1 Ridgecrest earthquake time.

Moving Time-Window Cross-Correlation Analysis

In this study, we use the moving time-window cross-correlation (MTWCC) technique to measure the subtle arrival time difference (TD) between the repeating events. We filter the three-component seismograms 1-10 Hz. A 0.5-second moving time window is used to compute CC. The original seismograms are interpolated 0.001s sampling. The slope of the decay versus time in the seismogram gives the fractional slowness change [*Schaff and Beroza*, 2004]. We also use a 1-second time window, starting from 0.2 second prior to the P & S predicted time to measure the P & S travel time difference between the two events within repeating event pairs. We only use the section of the seismogram pair with CC>0.9 to measure the slope.

The early state, within 20 days following M7.1 Ridgecrest EQ, healing process may be complicated. Fractional velocity changes are both positive and negative, perhaps because an early aftershock sequence occurred around that area.

Our results of the on-fault stations measurement indicate the velocity increase between 10 days before main shock and 40 days after are small, smaller or about 1% for both P and S waves.

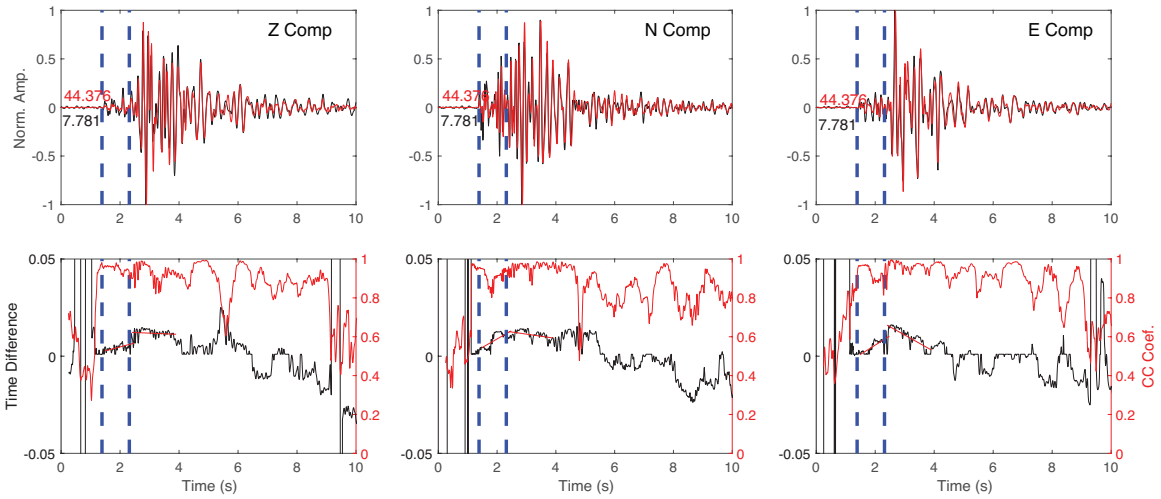

Figure 4. Examples of MTWCC for the three components. One events occurred about 8 days following the M7.1 mainshock and the other one occurred about 36.5 days later. (Top) panel shows the comparison of the seismograms with the black dashed lines marking the P and S arrival time. (Bottom) panel shows the DT and CC coefficients vary with time. Black lines show the DT and red lines show the CC coefficient. The best linear-fitting lines for the DT variations with time are marked with red lines following P and S waves.

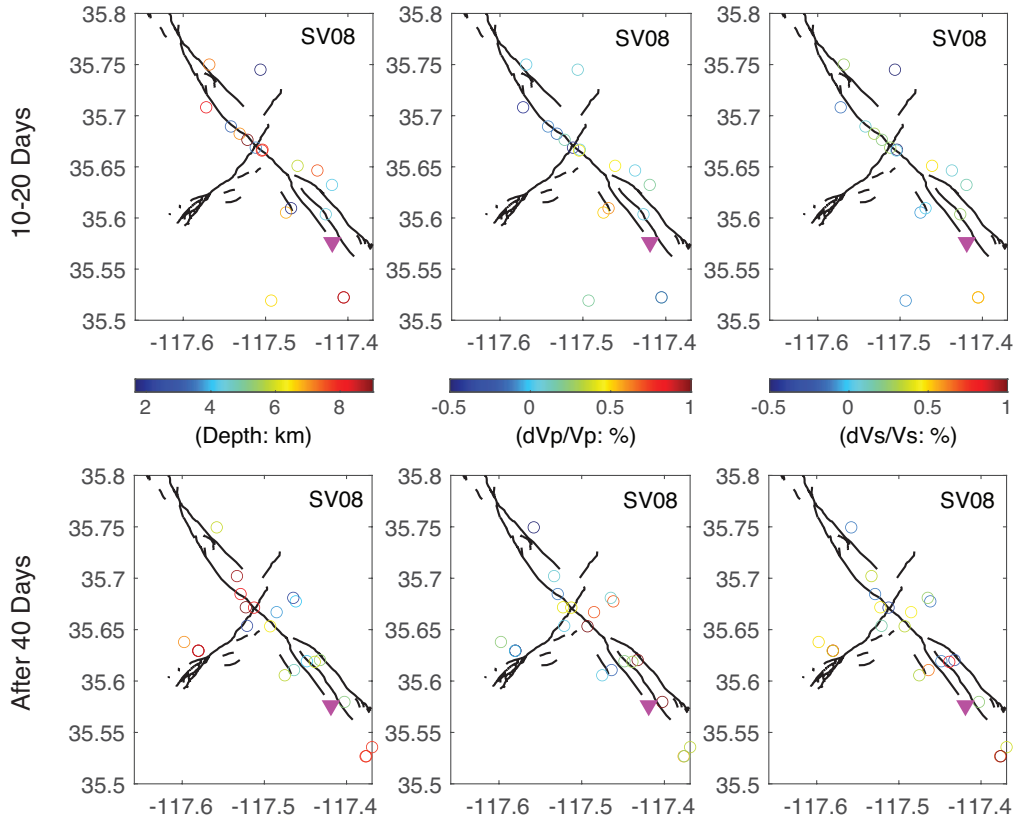

Figure 5. The fractional velocity change measured from slope of the decay versus time for station SV08. The top panel shows the depth distribution and velocity changes for the first event occurring time within 10 days following M7.1 mainshock and the second event occurring within 10 to 20 days. The bottom panel shows the depth distribution and velocity changes for the second events occurring after 40 days.

Reference

1. Li, Z., and Z. Peng (2016), An automatic phase picker for local earthquakes with predetermined locations: Combining a signal-to-noise ratio detector with 1D velocity model inversion, *Seismol. Res. Lett.*, 87(6),
2. Qiu, H., Ben-Zion, Y., Catchings, R. D., Goldman, M. R., Allam, A. A., & Steidl, J. H. (2020, 07). Detailed seismic imaging of the Mw7.1 Ridgecrest earthquake rupture zone from data recorded by dense linear arrays. Poster Presentation at 2020 SCEC Annual Meeting.
3. Schaff, D. P., and Beroza, G. C. (2004). Coseismic and postseismic velocity changes measured by repeating earthquakes. J. Geophys. Res., 109, B10302.
4. Snieder, R., & Vrijlandt, M. (2005). Constraining the source separation with coda wave interferometry: Theory and application to earthquake doublets in the Hayward fault, California. Journal of Geophysical Research: Solid Earth, 110(4), 1–15.
5. Trugman, D. T., Z. E. Ross, and P. A. Johnson (2020). Imaging Stress and Faulting Complexity Through Earthquake Waveform Similarity. Geophys. Res. Lett., 47 (1), e2019GL085888,
6. Xu, X., Sandwell, D. T., and Smith_Konter, B. (2020). Coseismic Displacements and Surface Fractures from Sentinel_1 InSAR: 2019 Ridgecrest Earthquakes. Seismol. Res. Lett.